

AB-891 941 NAVAL ACADEMY ANNAPOLIS MD  
DEEP LEVEL TRANSIENT SPECTROSCOPY AS AN EXPERIMENTAL TECHNIQUE. (U)  
JUN 80 S L SPEHN  
NSNA-TSPR-109

F/G 7/4

UNCLASSIFIED

NL

1 of 1  
SMA  
C-100

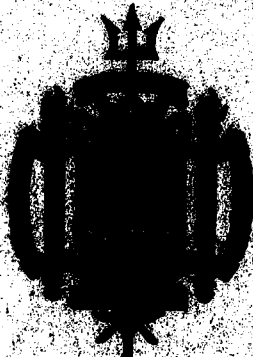
END  
DATE  
EN MED  
1-81  
DTIC

AD A091941

LEVEL  
A TRIDENT SCHOLAR  
PROJECT REPORT

NO. 43

DEEP LEVEL TRANSIENT SPECTROSCOPY  
AS AN EXPERIMENTAL TECHNIQUE



DTIC  
ELECTE  
S NOV 24 1980  
D

E -

UNITED STATES NAVAL ACADEMY  
ANNAPOLIS, MARYLAND

1980

## UNCLASSIFIED

SECURITY CLASSIFICATION OF THIS PAGE (When Data Entered)

REPORT DOCUMENTATION PAGE		READ INSTRUCTIONS BEFORE COMPLETING FORM
1. REPORT NUMBER U.S.N.A. - TSPR; no. 109 (1980)	2. GOVT ACCESSION NO. AD-A094 949	3. RECIPIENT'S CATALOG NUMBER
4. TITLE (and Subtitle) DEEP LEVEL TRANSIENT SPECTROSCOPY AS AN EXPERIMENTAL TECHNIQUE	5. TYPE OF REPORT & PERIOD COVERED Final: 1979/1980	
7. AUTHOR(s) Stephen Lester /Spehn	6. CONTRACT OR GRANT NUMBER(s) ① Final Rept. 1979-1980	
9. PERFORMING ORGANIZATION NAME AND ADDRESS United States Naval Academy, Annapolis.	10. PROGRAM ELEMENT, PROJECT, TASK AREA & WORK UNIT NUMBERS ⑩ 46.1	
11. CONTROLLING OFFICE NAME AND ADDRESS United States Naval Academy, Annapolis.	12. REPORT DATE ⑪ 5 June 1980	
14. MONITORING AGENCY NAME & ADDRESS (if different from Controlling Office) ⑭ US NA-TSPR-109	13. NUMBER OF PAGES 42	
16. DISTRIBUTION STATEMENT (of this Report) This document has been approved for public release; its distribution is UNLIMITED.	15. SECURITY CLASS. (of this report) UNCLASSIFIED	
17. DISTRIBUTION STATEMENT (of the abstract entered in Block 20, if different from Report) This document has been approved for public release; its distribution is UNLIMITED.	15a. DECLASSIFICATION/DOWNGRADING SCHEDULE	
18. SUPPLEMENTARY NOTES Accepted by the U. S. Trident Scholar Committee.		
19. KEY WORDS (Continue on reverse side if necessary and identify by block number) Spectroscopy Spectrum analysis Semiconductors	⑩	
20. ABSTRACT (Continue on reverse side if necessary and identify by block number) Deep Level Transient Spectroscopy (DLTS) is rapidly becoming the most popular method of studying defect trapping states in semiconductors. DLTS is sensitive, rapid, and straightforward to analyze; it is able to distinguish between traps of different energy levels as well as different capture cross sections; it is versatile in that it can provide any desired information on a given defect and it is able to cover a large spectrum of energy levels. DLTS can be used on any type of semiconductor with little or no change in system	OVER	

UNCLASSIFIED

SECURITY CLASSIFICATION OF THIS PAGE(When Data Entered)

20.

CONTINUED

setup. This makes it both a ~~very~~ convenient and ~~a very~~ powerful technique. This report ~~is an in-depth study of~~ the DLTS technique, introduced in this report is a mathematical model of the DLTS data analysis which until now has been somewhat limited in scope. This analysis is considered under a wide range of system setups and its effects are graphically shown in the Appendix. The source of error which causes the greatest uncertainty in results in DLTS is found to be the accuracy with which the applied phase shift can be measured. The results are found to vary by one percent per degree of phase shift. The system is then used to evaluate trapping states in a sample of Silicon and a sample of GaAlAs. For the Silicon the Energy Level is .433 eV with a prefactor of  $1.11 \times 10^7$ . For the GaAlAs the Energy Level is .59 eV with a prefactor of  $5.24 \times 10^7$ . Due to limitations of the DLTS apparatus it was not possible to determine the capture cross section of these samples. An electronic circuit is currently being developed to overcome this difficulty.

0 - 0

10 to the 7th power.

5.24 million.

UNCLASSIFIED

SECURITY CLASSIFICATION OF THIS PAGE(When Data Entered)

U.S.N.A. - Trident Scholar project report; no. 109 (1980)

DEEP LEVEL TRANSIENT SPECTROSCOPY  
AS AN EXPERIMENTAL TECHNIQUE

A Trident Scholar Project Report

by

Midshipman Stephen L. Spehn, Class of 1980  
U. S. Naval Academy  
Annapolis, Maryland

Robert N. Shelby  
Advisor: Prof. Robert N. Shelby

Physics Department

Accepted for Trident Scholar Committee

Chairman

Chairman

5 June 1980

Date

Accession For	
NTIS GRA&I	<input checked="" type="checkbox"/>
DDC TAB	<input type="checkbox"/>
Unannounced	<input type="checkbox"/>
Justification _____	
By _____	
Distribution _____	
Availability Codes _____	
Dist.	Avail and/or special
A	

### Abstract

Deep Level Transient Spectroscopy (DLTS) is rapidly becoming the most popular method of studying defect trapping states in semiconductors. DLTS is sensitive, rapid, and straightforward to analyze. It is able to distinguish between traps of different energy levels as well as different capture cross sections. It is versatile in that it can provide any desired information on a given defect and it is able to cover a large spectrum of energy levels. DLTS can be used on any type of semiconductor with little or no change in system setup. This makes it both a very convenient and a very powerful technique. This report is an in-depth study of the DLTS technique. Introduced in this report is a mathematical model of the DLTS data analysis which until now has been somewhat limited in scope. This analysis is considered under a wide range of system setups and its effects are graphically shown in the Appendix. The source of error which causes the greatest uncertainty in results in DLTS is found to be the accuracy with which the applied phase shift can be measured. The results are found to vary by one per cent per degree of phase shift. The system is then used to evaluate trapping states in a sample of Silicon and a sample of GaAlAs. For the Silicon the Energy Level is .433 eV with a prefactor of  $1.11 \times 10^7$ . For the GaAlAs

the Energy Level is .59 eV with a prefactor of  $5.24 \times 10^6$ . Due to limitations of the DLTS apparatus it was not possible to determine the capture cross section of these samples. An electronic circuit is currently being developed to overcome this difficulty.

### Acknowledgment

Even though this report bears my name, I am by no means the sole person responsible for all the work that went into its culmination. I drew upon the knowledge and skills of some very talented people. I would like to thank them for all the help that they so kindly provided me.

In the area of technical support I would like to thank three people. The first is Mr. Richard Krebs who helped me with the metalworking aspect of my apparatus. Secondly, I thank Mr. Charles Stump for allowing me to invade his workbench with a jungle of electronics. Mr. Stump also provided me with some insight into the Black Art of stabilizing Op Amps. And my special thanks go to Mr. Fred Wasem who personally supervised the construction of my equipment.

The man responsible for the special computer analysis of my Lock-In Amplifier model was Capt. R. J. Kimble. His intimate knowledge of the computer reduced my work on the computer to a nearly bearable amount of time.

But the man who deserves most of the credit is my Trident Advisor, Prof. Robert N. Shelby. Without Prof. Shelby's constant guidance and counsel none of my work would have been possible. He kept me abreast of all the newest developments in the field. He instructed me on the lesser known aspects of the experimental technique

under study. He cautioned me to question everything so that I would not duplicate the mistakes of others. He was my harshest critic and my strongest supporter. But most important, he gave me the strength to maintain my sanity throughout this whole affair.

Stephen L. Spehn

## TABLE OF CONTENTS

Abstract . . . . .	1
Acknowledgement . . . . .	3
Table of Contents . . . . .	5
Index to Figures . . . . .	6
I. Introduction . . . . .	7
II. Semiconductor Theory . . . . .	9
II-1. Electron Energy Levels . . . . .	9
II-2. Crystalline Defects . . . . .	11
II-3. Emission Rate . . . . .	13
II-4. Capture Cross Section . . . . .	16
III. Semiconductor Material . . . . .	18
IV. Experimental Theory . . . . .	20
IV-1. Transient Capacitance . . . . .	20
IV-2. Equipment Setup . . . . .	22
IV-3. Lock-In Amplifier Operation . . . . .	23
V. Experimental Results . . . . .	33
VI. Summary . . . . .	38
References . . . . .	39
Appendix . . . . .	40

## INDEX TO FIGURES

Figure	Page
II.1. Electron Energy Levels . . . . .	9
II.2. Electron Transitions . . . . .	12
IV.1. Trapping of Majority Carriers . . . . .	21
IV.2. Equipment Setup . . . . .	23
IV.3. Input to Lock-In . . . . .	24
IV.4. Block Diagram of HR-8 . . . . .	25
IV.5. Voltage Gain of Signal Tuned Amplifier . . .	26
IV.6. $1/x$ vs. Frequency for $\tau = 1.6\text{msec.}$ . . . . .	30
IV.7. Emission Rate vs. Phase Shift . . . . .	31
IV.8. Emission Rate vs. Relative Hold Time . . . .	32
V.1. Lock-In Output vs. Temperature . . . . .	35
V.2. Energy Plot for Silicon . . . . .	36
A.1. Emission Rate vs. $f$ for $\Phi = 0$ . . . . .	40
A.2. Third Order Fit for Emission Rate Ratio . .	41
A.3. Third Order Fit for Inverse Emission Ratio . . . . .	42

## Introduction

Virtually all of modern electronics is made possible by the utilization of the physical properties of semiconductors. These properties are governed primarily by the nature of the dopants planted in the crystalline structure of the semiconductor. The Energy Levels and capture cross sections of these dopants have been accurately determined by rather straightforward experimental techniques such as Thermally Stimulated Current (TSC) or Thermally Stimulated Capacitance (TSCAP). In addition to these methods, luminescence studies have proved useful in the characterization of these shallow Energy States. But these techniques prove unacceptable in the study of crystalline defects, which generally have a deeper Energy Level than common dopants.

Many of these defects act as hole or electron trapping states depending on their Energy Level and capture cross sections. As such they contribute a great deal to the electronic properties of the semiconductor device. They provide the primary mechanism for the thermal generation of electrons. These defects are responsible for the complexing of planted dopants, thus altering the designed electronic properties of the device. The electro-luminescent characteristics of the device are also changed by the kinematics of these defects. For

these reasons there is a great deal of interest in the study of defect trapping states. One of the leaders in this field is Lang<sup>1</sup>, who has developed an experimental technique known as Deep Level Transient Spectroscopy (DLTS).

DLTS incorporates a high frequency digital capacitance meter to measure the change in capacitance due to trapped charge carriers in the depletion region. By selectively measuring the time rate of change of this trapped charge it produces a signal which is proportional to the concentration of the trapped charge. By doing a thermal scan of the emission rate of the trapped charge it is possible to determine the Energy Levels, concentration profile, and electron and hole capture cross sections of these trapping states. DLTS is far superior to TSC and TSCAP in the areas of noise immunity, sensitivity, and range of observable Energy Levels.

In Chapter II. I review the basic theory of semiconductors and their related defects. Chapter III. goes into more detail of the semiconductors used in my study, Silicon and GaAlAs. The experimental technique itself is covered in Chapter IV. The application of this technique (DLTS) is covered in Chapter V. And the results of the experiment are discussed in Chapter V. Chapter VI.. summarizes the important aspects of this work.

## Chapter II.

III-1. Electron Energy Levels

There exists no hard definition of a semiconductor. It is generally accepted, however, that a semiconductor is a crystalline solid possessing electronic Energy bands similar to those in Figure II.1(b). The important characteristics which distinguish between a metal, a semiconductor, and an insulator are the Energy Gap and the Fermi Energy. As seen in Figure II.1, the Fermi Energy is above the Conduction Band Energy for a metal, so the Conduction Band always contains states filled with electrons.

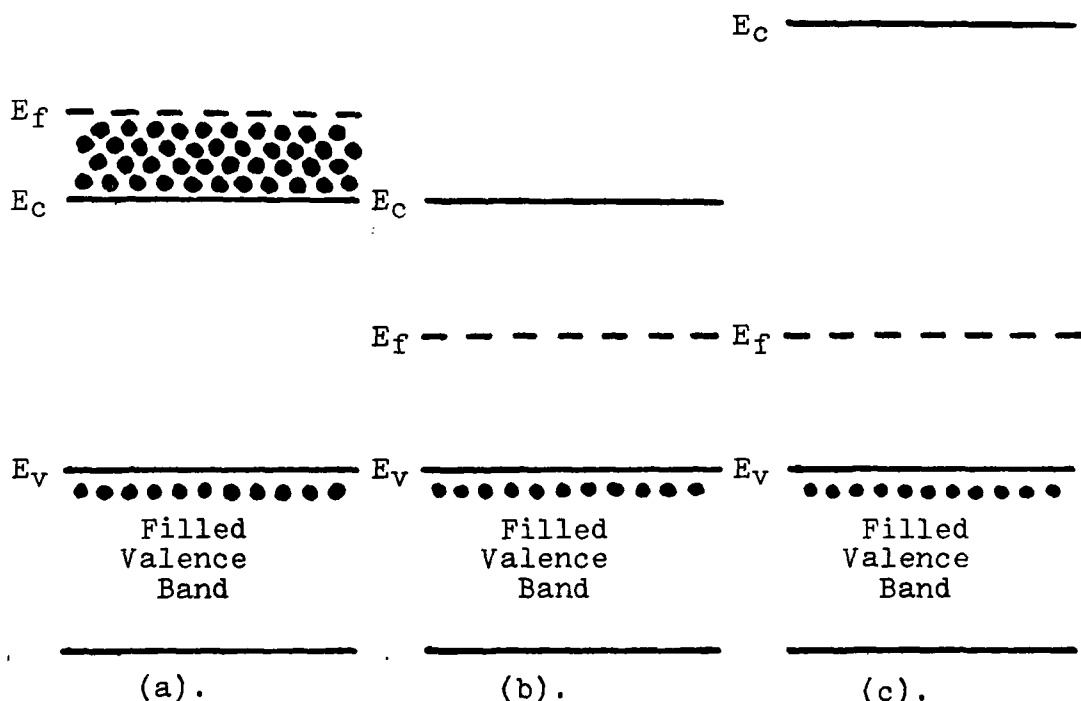


Figure II.1. Energy Levels for (a). a metal; (b). a semiconductor; and (c). an insulator.

For a semiconductor the Fermi Energy is somewhere in the Band gap and the Band gap Energy is of the order of 1 to 3 eV. An insulator is similar to a semiconductor except that the Band gap Energy is much greater; about 5 to 10 eV. The Band gap is the Energy range between the Conduction and the Valence Bands.

But a pure semiconductor is almost useless for it merely exhibits the properties of a temperature dependent resistor. So in order to control the properties of the device impurity atoms are added to the semiconductor. These impurities, or dopants, are usually from the III or V column of the Periodic Table of Elements. When these dopants ionize they create either a hole or a conduction electron depending on whether they are acceptors or donors, respectively. These impurities are mostly ionized even at very low Temperatures because their Energy states lie close to either the Conduction Band for donors or the Valence Band for acceptors. These dopants thus create excess majority or minority carriers depending on the type of dopant and whether the semiconductor is an n or p type. If there are more donors than acceptors then the material is n type; if there are more acceptors than donors then the material is p type. By controlling the spatial concentration of these dopants it is possible to tailor fit a semiconductor device to the specific requirements of the Design Engineer.

### II-2. Crystalline Defects

Crystalline defects, as opposed to dopant impurities, are neither easily controlled nor very well understood. There have been several theories about their formation and physical properties but none have been able to predict the Energy Levels and capture cross sections found in various experimental results.<sup>2</sup> Defect trapping states also have the nasty habit of changing their electronic parameters with a change of Temperature. Sometimes the defect changes its nature completely, thus permanently altering the operating characteristics of the semiconductor device.

Despite their unpredictability, defects exhibit many of the same properties as dopants. Like dopants they are basically Energy states for holes or electrons located somewhere in the Energy gap. As such they are governed by the same thermodynamic laws as the dopants. From a basic consideration of Thermodynamics it is possible to predict the defect's most important properties.

As shown in Figure II.2 there are four distinct processes which govern the trapping of electrons (or holes) by defect states. The first process,  $r_1$ , concerns the rate of transition of the electrons from the Conduction Band to the trapping state. The second process,  $r_2$ , is the rate at which electrons are emitted from the trapping state back to the Conduction Band. The third

and fourth processes,  $r_3$  and  $r_4$ , are the rates at which electrons are captured from and emitted to the Valence Band. If the time rate of change of the number of trapped electrons is zero, then it is evident that

$$r_1 - r_2 = r_4 - r_3$$

This is the condition of Steady State. But Steady State is generally a condition of non-equilibrium in which the sum of the processes have a constant result. For instance, if  $r_1 = r_4$  and  $r_2 = r_3$ , but  $r_1$  is greater than  $r_2$ , then the net result is a transfer of electrons from the Conduction Band to the Valence Band. This, certainly, is not possible for a system in equilibrium.

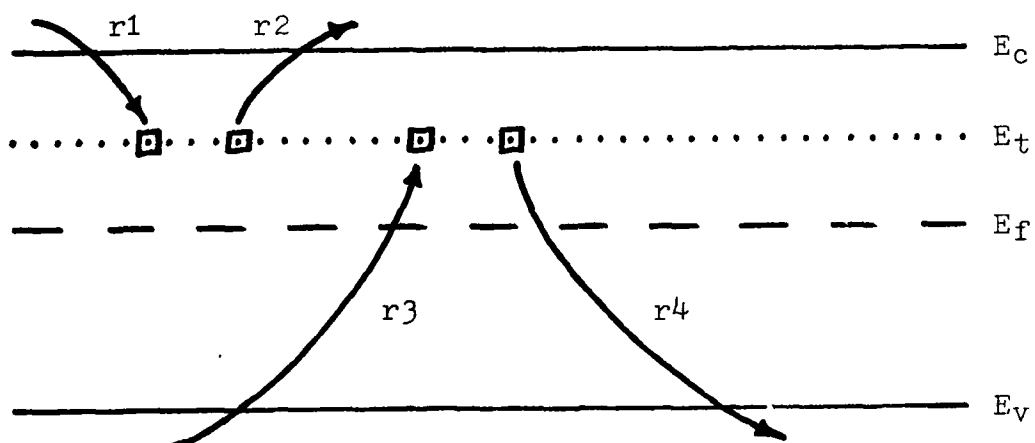


Figure II.2. The four transition rates governing the occupation of a trapping state.

With a system in thermal equilibrium it obeys an even more fundamental law than the ones governing Steady State.

This Law is the Principle of Detailed Balance and it states that under the condition of equilibrium, every process is exactly balanced by its inverse. Thus, in equilibrium,  $r_1 = r_2$  and  $r_3 = r_4$ . In DLTS it will be very important to distinguish between the conditions of Steady State and equilibrium.

### II-3. Emission Rate

By considering a system in equilibrium it is possible to determine the emission rate for an assembly of traps. I will do this for an n type semiconductor material and consider only electron trapping states.

The electron capture rate,  $r_1$ , is proportional to the capture cross section of the defect, the thermal velocity of the electrons, The number of electrons in the Conduction Band and the number of empty trapping states. The electron emission rate,  $r_2$ , is proportional to the number of filled trapping states and the rate at which a single trap emits electrons. In equilibrium these two rates exactly balance each other;  $r_1 = r_2$ . In addition, by using Fermi-Dirac statistics, the population of the trapping states can be precisely determined. The population is simply the product of the concentration of traps and their Fermi function. The Fermi function relates the probability of occupation to the Energy Level. The Fermi function is also dependent on temperature.

A list of important parameters is given below.

$\sigma$	capture cross section
$v$	thermal velocity
$n$	number of electrons in the Conduction Band
$N_t$	total number of trapping states
$e$	electron emission rate of trapping states
$f(E)$	Fermi function

$$\text{where } f(E_t) = \frac{1}{1 + e^{(E_t - E_f)/kT}} \quad (\text{II-1})$$

The capture and emission rates are given by

$$r_1 = \sigma v n [1 - f(E_t)] N_t \quad (\text{II-2})$$

$$\text{and } r_2 = N_t e f(E_t) \quad (\text{II-3})$$

Setting  $r_1$  equal to  $r_2$  gives

$$\sigma v n [1 - f(E_t)] N_t = N_t e f(E_t)$$

Solving for the emission rate,  $e$ , yields

$$e = \sigma v n \frac{1 - f(E_t)}{f(E_t)} \quad (\text{II-4})$$

We can now get an expression for  $e$  by combining Equations (II-1) and (II-4).

$$e = \sigma v n e^{(E_t - E_f)/kT} \quad (\text{II-5})$$

The number of electrons in the Conduction Band,  $n$ , can be approximated by an effective density of states,  $N_c$ , times the Maxwell Boltzmann distribution. This distribution

is an approximation of the Fermi function in which  $E_c - E_f$  is very much greater than  $kT$ .

$$n = N_c e^{(E_f - E_c)/kT} \quad (\text{II-6})$$

Now, putting Equation (II-6) into Equation (II-5) and letting  $\Delta E = E_c - E_t$ , we end up with the standard expression for the electron emission rate;

$$e = \sigma v N_c e^{-\Delta E/kT} \quad (\text{II-7})$$

Using the expressions for  $v$  and  $N_c$ ;

$$v = \left[ \frac{3kT}{m^*} \right]^{\frac{1}{2}} \quad (\text{II-8})$$

$$\text{and} \quad N_c = 2 \left[ \frac{2 m^* kT}{h^2} \right]^{\frac{3}{2}} \quad (\text{II-9})$$

So the final expression for  $e$  is

$$e = A T^2 e^{-\Delta E/kT} \quad (\text{II-10})$$

where  $A$  is a very weak function of Temperature.

DLTS is a sophisticated experimental technique which determines the emission rate,  $e$ , as a function of Temperature,  $T$ . Knowing the emission rate at several different Temperatures it is relatively easy to find  $A$  and  $\Delta E$  by expressing Equation (II-10) in the form

$$\ln\left(\frac{T^2}{e}\right) = \frac{\Delta E}{kT} - \ln A \quad (\text{II-11})$$

By doing several thermal scans at different settings for the emission rate window, the Energy Level of the trap can be determined by plotting  $\ln(T^2/e)$  vs.  $1/T$ . The Energy Level is then the slope times the Boltzmann constant and  $A$  is the inverse of the exponential of the intercept.

#### II-4. Capture Cross Section

In some applications (such as electroluminescence) it is necessary to determine the capture cross section of the active trapping states. To see how DLTS accomplishes this it is necessary to understand the relationship between the number of filled trapping states and the output signal of the DLTS apparatus.

In Chapter IV. it will be shown that the output signal of the DLTS equipment is directly proportional to  $\Delta C$ ; where  $\Delta C$  is the change in junction capacitance due to the presence of filled electron trapping states. And the change in junction capacitance is directly proportional to the number of trapping states which are currently filled with electrons. By applying a Voltage pulse across the junction to fill these trapping states, their population is changed according to the length of the applied pulse. This change can be determined by using Equations (II-2) and (II-3) under the conditions of Steady State. Thus the change in filled traps with respect to time is given by

$$\frac{dN}{dt} = r_1 - r_2$$

$$\text{so } \frac{dN}{dt} = \sigma v n \left[ 1 - f(E_t) \right] N_t - N_t f(E_t) e$$

Simplifying this expression and evaluating the integral yields the relationship between the length of the applied Voltage pulse and the population of the defect trapping state. For this expression  $N(t)$  is the

population of the trapping state at time  $t$ .

$$N(t) = N_0 [1 - e^{-t/\tau}] . \quad (\text{II-12})$$

$$\text{where } \frac{1}{\tau} = \sigma v n + e$$

For this expression I am considering only an electron trap so that its interaction with the Valence Band is small and can be neglected.

Since the output of the Lock-In Amplifier,  $L(T)$ , is proportional to  $\Delta C$  which is proportional to  $N(t)$ , then, by varying the applied pulse length you change the magnitude of  $L(T)$ . A plot of  $\ln L$  vs.  $t$  will readily give a value for  $\tau$ . Knowing this and the emission rate will provide a value for the capture cross section.

## Chapter III.

The semiconductors used for measurements in this study were Silicon and GaAlAs. Silicon is the most common semiconductor used in modern devices. It has a Face Centered Cubic lattice structure with a basis of two atoms at  $(0,0,0)$  and  $(\frac{1}{4},\frac{1}{4},\frac{1}{4})$ . GaAlAs is much more complex than doped Silicon and thus requires a more detailed study. The purpose of this paper, however, is an in-depth study of the DLTS technique, and not of the specific semiconductors used in the study. As such only a brief description of the differences between the two materials will be presented.

Even though Silicon is used in state of the art electronic circuits, GaAs is swiftly becoming more popular in very specialized situations. This compound semiconductor is especially important in the microwave frequency range and in circuits utilizing optoelectronic devices such as injection lasers and Light-Emitting-Diodes (LED).

The different structures result in a more complex crystalline structure for GaAs as well as a larger Energy gap. The structure of GaAs makes the defects in it more stable than the same defects in Silicon due to obviously greater complexity in the movement of a defect in GaAs. As such we would expect GaAlAs to require higher temperatures

to change the defects. This increased complexity should also lead to a greater variety of defects in GaAlAs than that found in Silicon.

Other important differences include the much greater lattice strain per defect of GaAs as opposed to Si. Studies of radiation induced length-change and optical measurements of defects show that the related lattice relaxation effects are much stronger in GaAs than in Si. These relaxation effects have a profound influence on the behaviour of defects as nonradiative recombination centers (Lang and Henry 1975, Henry and Lang 1977).<sup>4</sup>

The behaviour of defects as trapping states, however, is basically the same for both GaAs and Si. The emission rates of traps in both substances obey Equation (II-10), and, as such, GaAs and Si are subject to the same method of analysis under the DLTS technique. In other words, DLTS can be used on any type of semiconductor with absolutely no change in the system setup or in the analysis of the data. This makes DLTS both very convenient and very powerful.

## Chapter IV.

IV-1. Transient Capacitance

The parameter which is actually measured in a DLTS run is the junction capacitance of the semiconductor device. For an abrupt junction the capacitance per unit area is

$$C = \frac{\epsilon_s}{x_d}$$

where  $C$  is the capacitance,  $\epsilon_s$  is the permittivity of the semiconductor, and  $x_d$  is the width of the depletion region. For this model it is evident that the junction capacitance is a function only of the width of the depletion region. But this is only true for the condition of Steady State. Deep Level Transient Spectroscopy (DLTS), as its name implies, measures the transient capacitance of the depletion region after the application of a majority or minority carrier pulse. I will treat only the case of the majority carrier pulse, as this is the method which I used in my study.

Consider an abrupt  $p^+$ - $n$  type junction. For this case the depletion region extends primarily into the  $n$  type region. When a quiescent reverse bias is applied the width of the depletion region is extended out past its equilibrium position. If a majority carrier pulse is applied, the traps in the depletion region fill up according to Equation (II-12). Then, when the applied bias is re-

turned to its quiescent value, the states depopulate according to Equation (II-10). This sequence of events is shown in Figure IV.1.

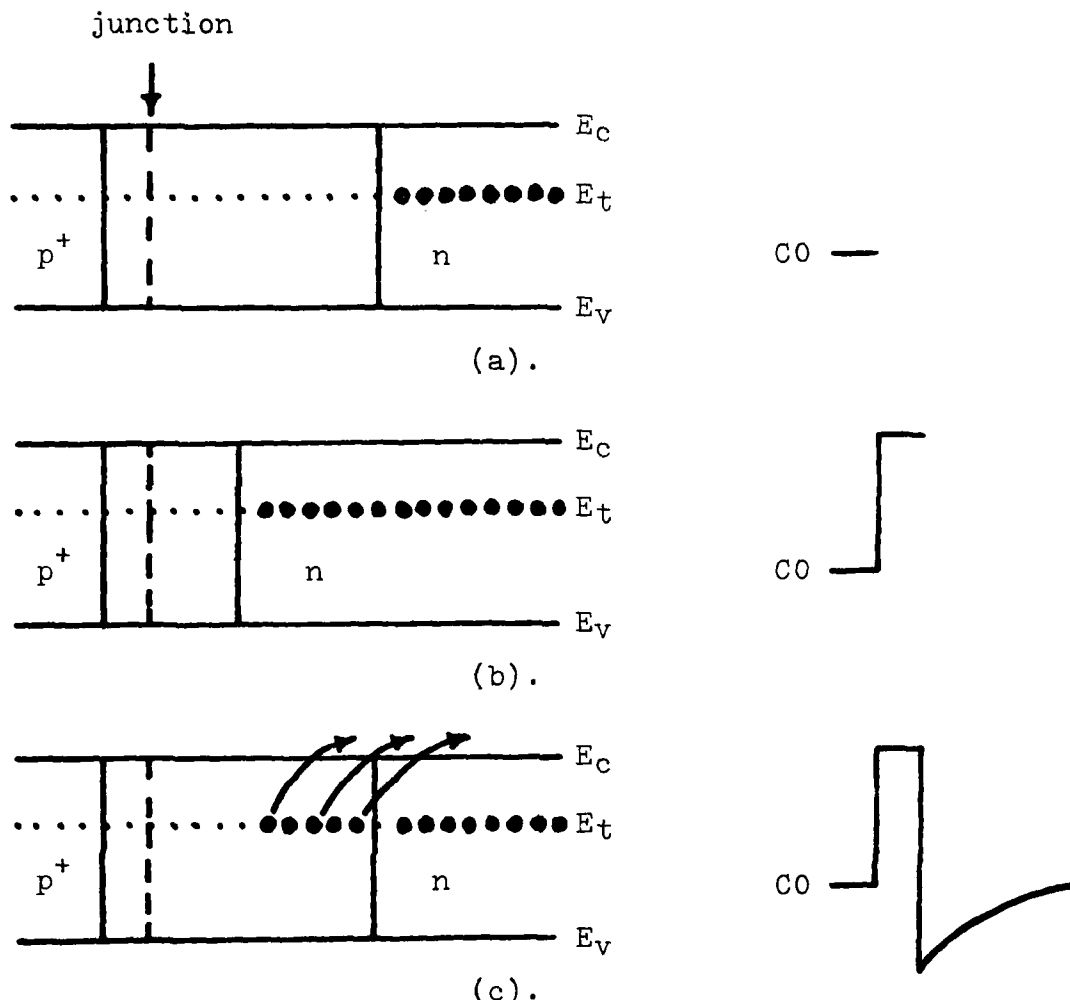


Figure IV.1. Trapping of majority charge carriers in the depletion region during a bias pulse transient.

The trapped charge in the depletion region affects the capacitance of the junction by reducing the total charge separation across the depletion region. After the

return to quiescent reverse bias, the trapped electrons remain in the depletion region until they are thermally emitted by the defects. This thermal emission is the same process which affects the population of the traps, since there are no free electrons for the trapping state to trap. Thus the capacitance is of the form of an exponential time decay.

#### IV-2. Equipment Setup

The equipment setup is shown in Figure IV.2. The heart of the equipment is the Switch and Control circuit. This circuit has a multitude of functions. It is triggered by the Lock-In Amplifier and, upon receipt of this trigger, it applies a majority carrier pulse to the semiconductor to populate the traps in the quiescent depletion region. During this time it also disconnects the capacitance meter from the sample to prevent this pulse from causing signal input overload to the meter. After the majority carrier pulse is removed, the circuit reconnects the sample to the capacitance meter. The recovery time of the capacitance meter after complete overload is about 1 millisecond. To compensate for this the Control circuit employs a Sample and Hold circuit. The circuit is held in the Hold mode from the beginning of the majority carrier pulse until about 1 msec after this pulse is removed. The signal is then fed through a linear

preamplifier to provide AC coupling to the Lock-In Amplifier. It should be noted that the function and design of the Switch and Control circuit has been continually improved upon since the beginning of the study. The current design for this circuit is still being developed and will be presented in a future paper.

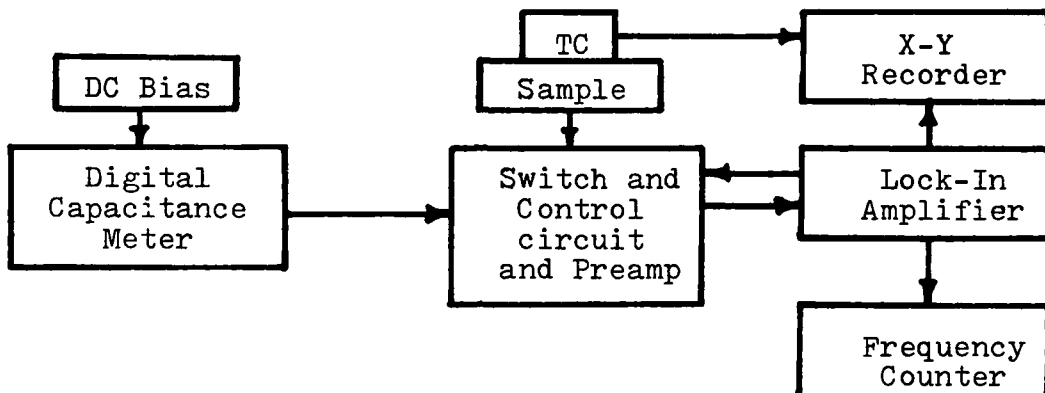


Figure IV.2. Equipment setup for DLTS.

DLTS systems can be setup using either a Dual Boxcar Integrator or a Lock-In Amplifier. But the Lock-In has a much better signal-to-noise ratio and thus is able to detect signals which would be either too weak or too noisy for the Boxcar Integrator. The analysis for the Boxcar Integrator, however, is much simpler than the computer analysis necessary for the Lock-In Amplifier. In addition, there is some disagreement over what is the correct analysis of data for the Lock-In Amplifier.

#### IV-3. Lock-In Amplifier Operation

Without a proper analysis of the Lock-In technique,

all previous results are subject to question. Yet it is difficult to critique previous published works, for most authors do not even discuss the method of analysis used. The few who do discuss it, do so in a very ambiguous manner. Thus there is currently no standard method of analysis used in this field of research. I will devote most of the rest of this chapter on a detailed method of analysis for the Lock-In technique. Then I will compare my method with the one proposed by Lang (1979).<sup>5</sup>

Figure IV.3. shows the decaying exponential which is the output of the Switch and Control circuit.

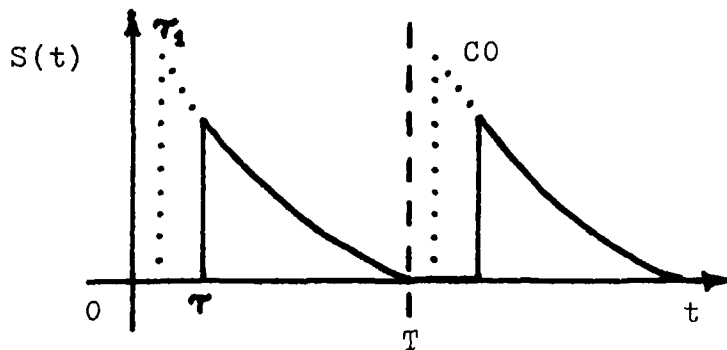


Figure IV.3. Input signal to the Lock-In Amplifier.

where  $T_1$  = length of the majority carrier pulse

$\tau$  = length of hold time

$T$  = period of system setup

As seen in Figure IV.3. the function  $S(t)$  is given by

$$S(t) = \begin{cases} 0 & 0 \leq t < \tau \text{ (IV-1.a)} \\ e^{t\tau_1} C_0 (e^{-et} - e^{-eT}) & \tau \leq t \leq T \text{ (IV-1.b)} \end{cases}$$

Expanding  $S(t)$  into a Fourier Series yields

$$S(t) = \frac{a_0}{2} + \sum_{n=1}^{\infty} \left[ a_n \cos 2\pi n \frac{t}{T} + b_n \sin 2\pi n \frac{t}{T} \right] \quad (\text{IV-2})$$

where  $a_0 = \frac{2}{T} \int_0^T S(t) dt$

$$a_n = \frac{2}{T} \int_0^T S(t) \cos 2\pi n \frac{t}{T} dt$$

and  $b_n = \frac{2}{T} \int_0^T S(t) \sin 2\pi n \frac{t}{T} dt$

This signal, after initial amplification by the preamplifier, is sent through a signal tuned amplifier. This amplifier provides a voltage gain which is highly sensitive to the frequency of the signal. Hence, for a Fourier Series, the gain is a function of the order of the harmonic (n). Figure IV.5. shows the gain as a function of harmonic for the PAR HR-8, used for this study.

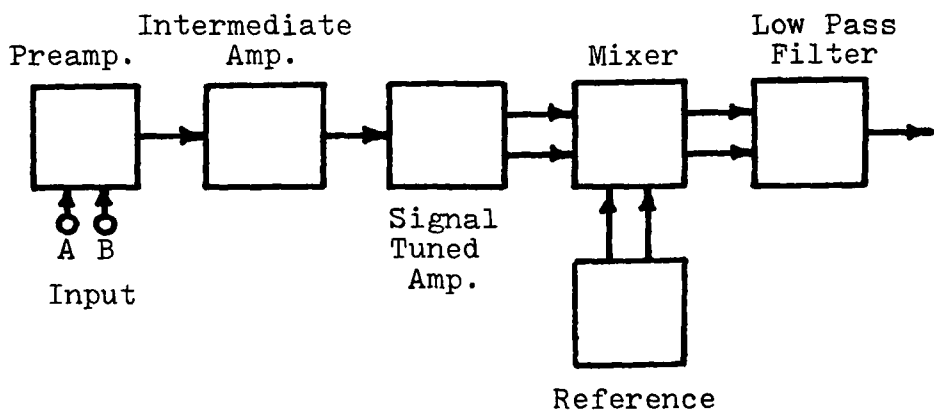


Figure IV.4. Block diagram of HR-8.

The output of the Signal Tuned Amplifier is thus

$$S'(t) = \sum_{n=1}^{\infty} g(n) \left[ a_n \cos 2\pi n \frac{t}{T} + b_n \sin 2\pi n \frac{t}{T} \right] \quad (\text{IV-3})$$

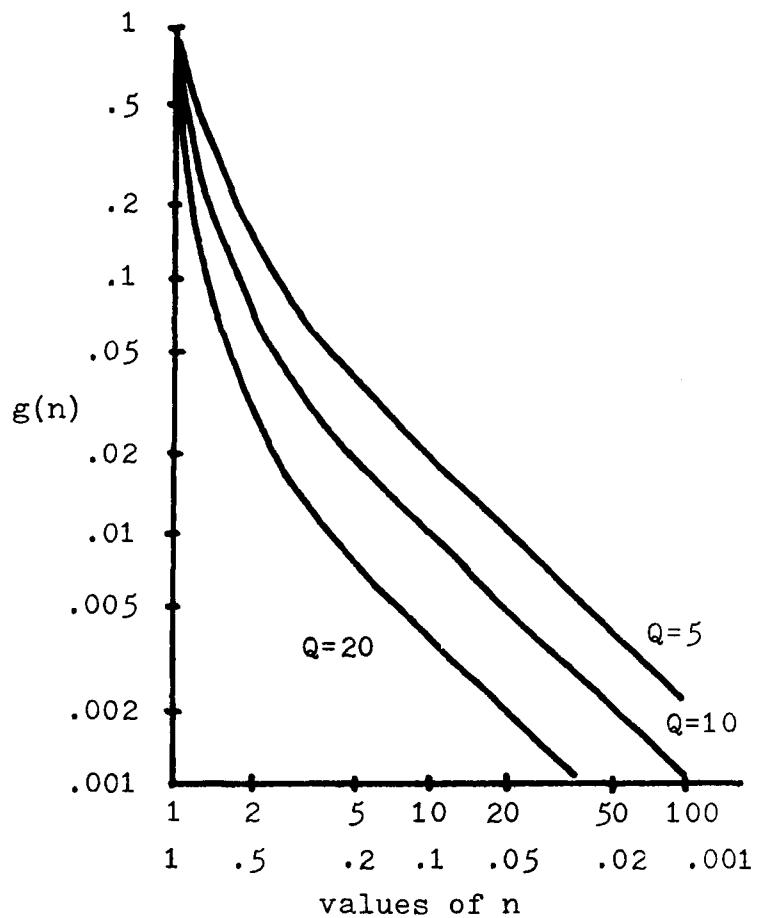


Figure IV.5. Relative voltage gain vs. harmonic for the Signal Tuned Amplifier.

The output of the Signal Tuned Amplifier is sent through a mixer which multiplies  $S'(t)$  by a synchronous square wave. This square wave can also be expanded into a Fourier Series given by

$$SW(t) = \sum_{m=0}^{\infty} \frac{4}{(2m+1)} \sin \left[ (2m+1) 2\pi \frac{t}{T} + \varphi \right]$$

where  $\varphi$  is the phase difference set into the mixer by the reference input. This adjustment is set by the front panel phase setting control on the HR-8.

The output of the mixer is a series of sum and difference components which are then sent through a low pass filter. The corner frequency of this filter is

$$f_c = \frac{1}{8TC}$$

where TC is the time constant set on the front panel of the HR-8. This expression is applicable for the 12 dB per decade rolloff setting.

Thus the low pass filter effectively screens out all components except for the time independent DC difference components. This filtering, combined with the highly frequency dependent Signal Tuned Amplifier, limits the output of the Lock-In (  $L(T)$  ) to just the coefficient of the fundamental Fourier component of the input signal.

The Lock-In output is thus

$$L(T) = \frac{2}{\pi} [a_1 \sin \varphi + b_1 \cos \varphi] \quad (IV-4)$$

Using the following definitions;

$$\varphi = fT \quad eT = x \quad \varphi_1 = f_1 T$$

and evaluating the coefficients with Equations (IV-1) and (IV-2) yields

$$L(T) = \frac{2}{\pi} C_0 e^{f_1 x} \left[ \begin{aligned} & \left[ \frac{2e^{-fx}}{x^2 + 4\pi^2} (x \cos 2\pi f - 2 \pi \sin 2\pi f) \right. \\ & \left. - \frac{2xe^{-x}}{x^2 + 4\pi^2} + \frac{e^{-x}}{\pi} \sin 2\pi f \right] \sin \varphi \\ & + \left[ \frac{2e^{-fx}}{x^2 + 4\pi^2} (x \sin 2\pi f + 2 \cos 2\pi f) \right. \\ & \left. - \frac{4\pi e^{-x}}{x^2 + 4\pi^2} + \frac{e^{-x}}{\pi} (1 - \cos 2\pi f) \right] \cos \varphi \end{aligned} \right] \quad (IV-5)$$

The emission rate window is found by setting the derivative of  $L(x)$  with respect to  $x$  equal to zero.

A comparison of the method presented here with the method proposed by Lang<sup>5</sup> is quite interesting. Lang sets out three different methods, each with its own definition of the phase shift. Each method, however, uses the same approximation for the operation of the Lock-In. Lang states that the Lock-In measures the amplitude and phase of the fundamental Fourier component of the transient input. He further states that the Lock-In output is the integral of the product of the square wave and this fundamental Fourier component. This integration approximation yields slightly different results compared to the method outlined previously.

In the lower limit both methods give the same result. This is for the case of zero majority carrier pulse length, zero hold time and zero phase lag. For this limit the expression reduces to

$$L(x) = \frac{4}{\pi} \text{Co} \frac{x(1-e^{-x})}{x^2+4\pi^2} \quad (\text{IV-6})$$

But this limit is the idealized case and is no better than a zeroth order approximation. As we move towards longer pulse lengths and greater hold times the two methods begin to deviate. This discrepancy arises due to Lang's approximation of the operation of the Lock-In.

Lang demonstrates his method by applying it to a few specific cases. Probably his most telling application is a plot of emission rate window versus frequency for a hold time of 1.6 msec. For this case the two methods are in excellent agreement. Both result in the plot shown in Figure IV.6. They are also in relatively good agreement concerning the emission rate window as a function of phase shift for a constant hold time,  $\tau$ . This case is shown in Figure IV.7. The only real discrepancy arises when the gate off time becomes an appreciable fraction of the period. Then Lang's method starts to break down due to his approximation of the operation of the Lock-In Amplifier.

A complete treatment of my method of analysis was done on the computer with the more important results being shown graphically in the Appendix. As seen in Figure IV.8. the worst problem arises in the determination of the phase shift. Figure IV.8. shows that this uncertainty results in an error of about one percent per degree phase shift error. This can become a considerable source of error if the Lock-In is not equipped with a very accurate 10 turn adjustment control for the applied phase shift.

Using this method of analysis it is now possible to make experimental data runs and to be certain of the results to within a few percent.

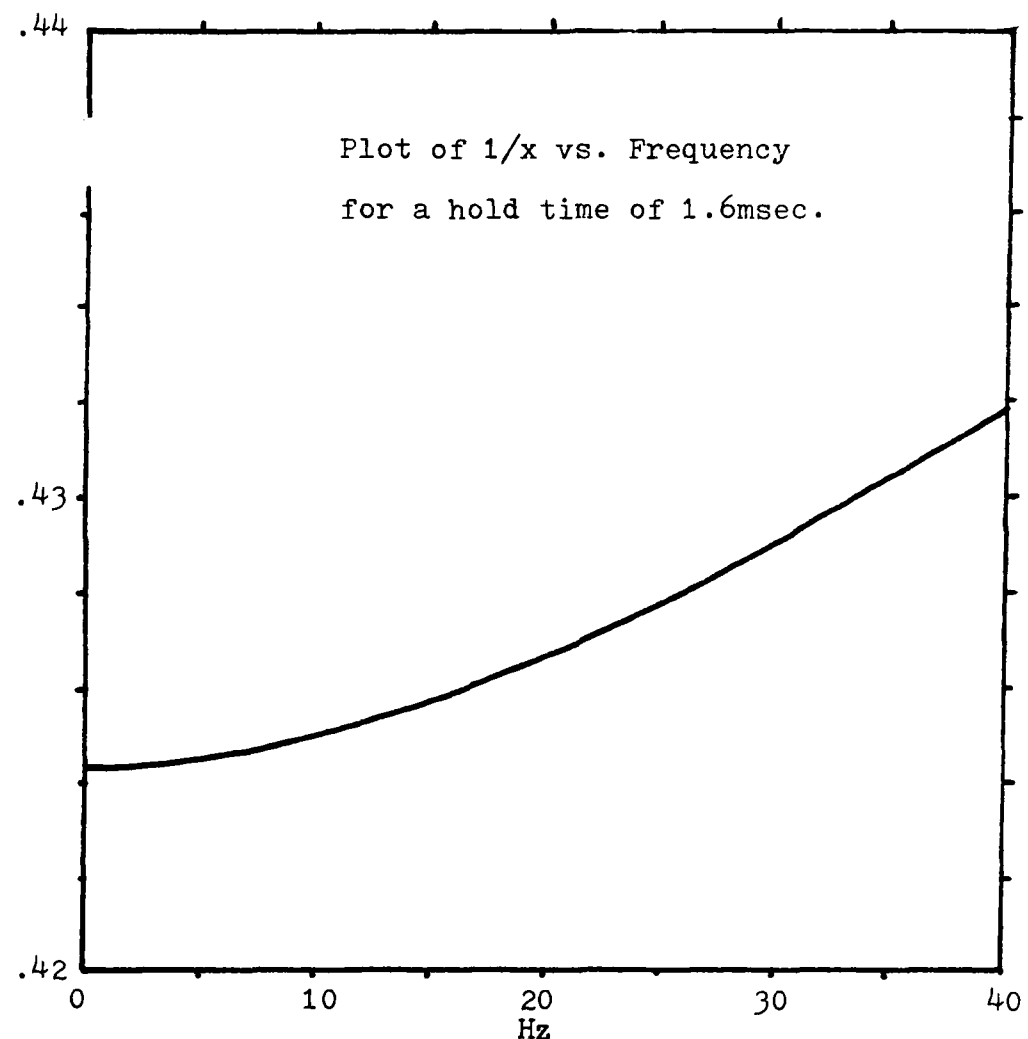


Figure IV.6. Plot of inverse emission rate vs. Frequency for a hold time of 1.6 msec.

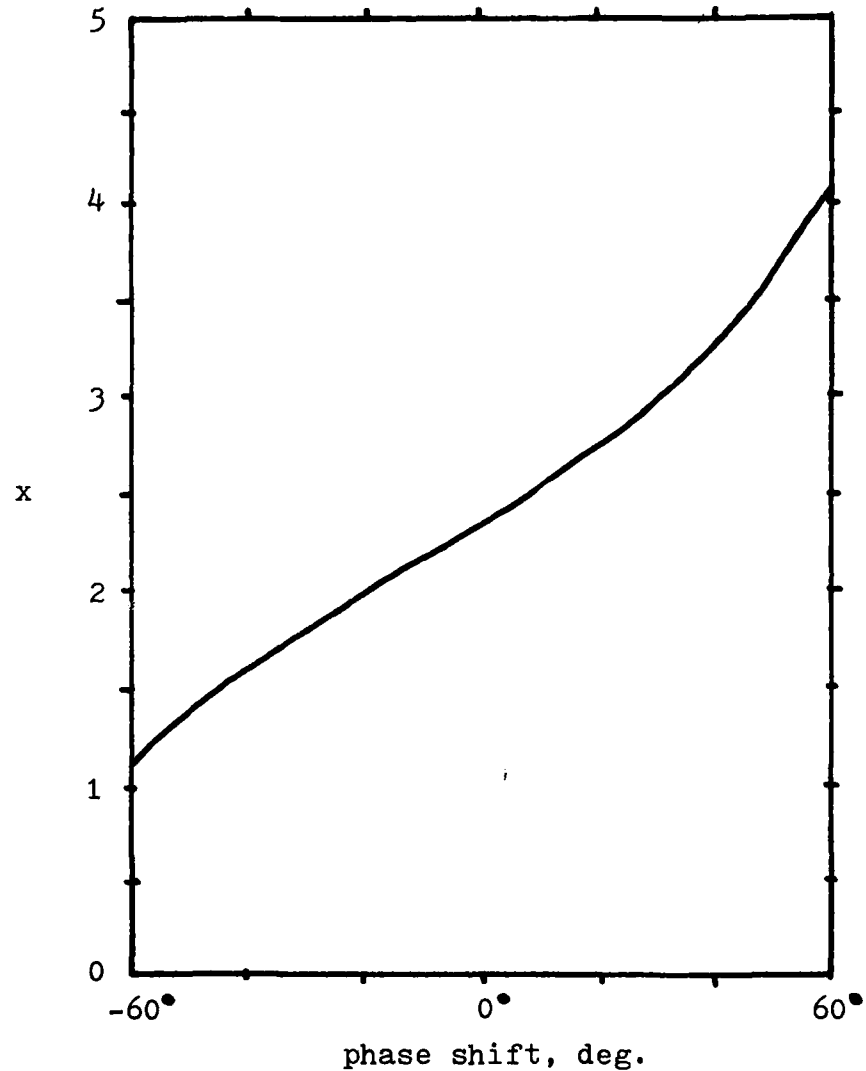


Figure IV.7. Plot of relative emission rate vs. phase shift for zero pulse length and zero hold time.

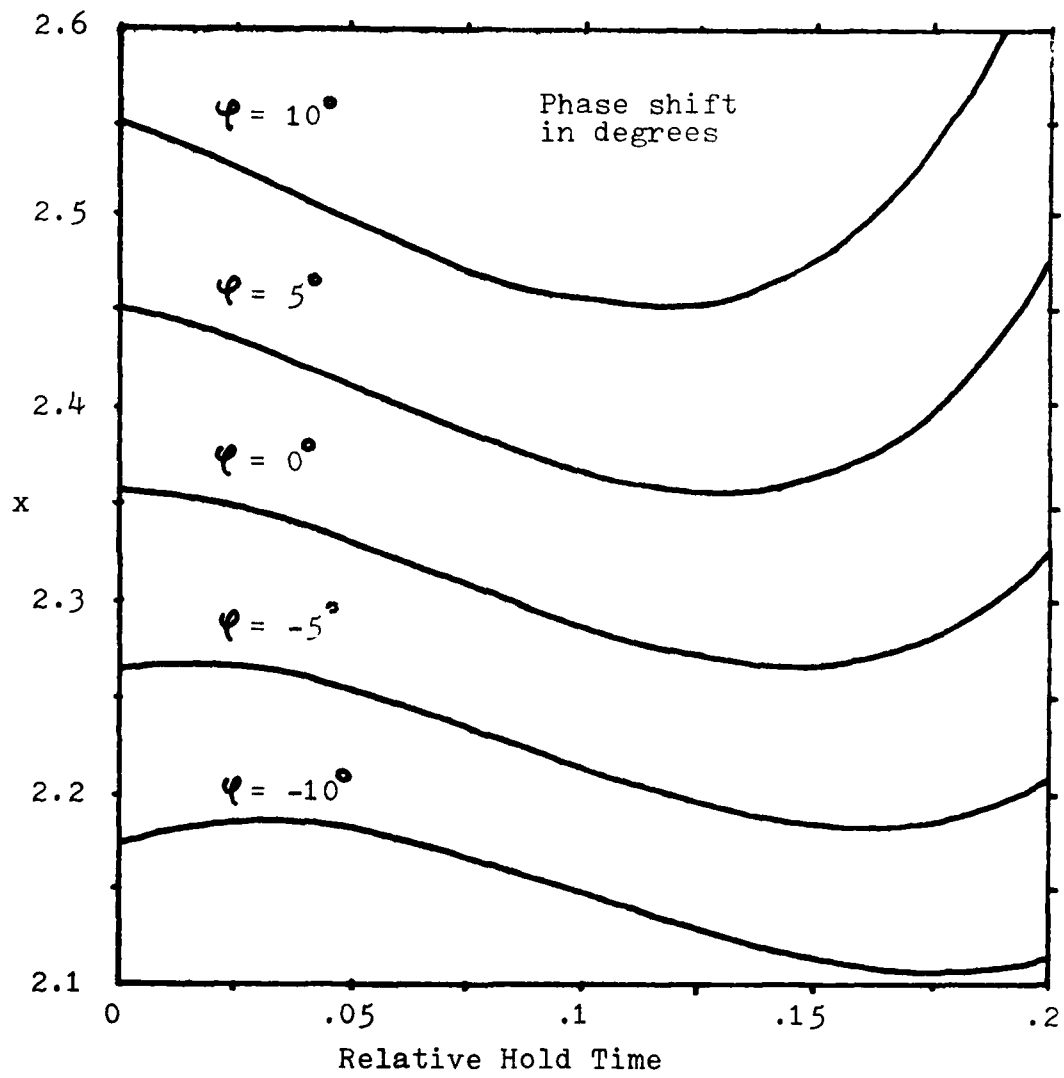


Figure IV.8. Plot of relative emission rate vs. relative Hold time for five different values of phase shift,  $\varphi$ .

## Chapter V.

In this section I will detail the procedure used and the intermediate data for the defects in Si. Since the method of analysis is exactly the same for both Si. and GaAlAs, I will then only present the observed data and the results of the runs done on the GaAlAs.

The important parameters set into the HR-8 Lock-In Amplifier are as follows:

Phase — 0°

Calibrate — 100 mV

Time Constant — 1 sec. 12 dB/oct.

Mode — INTERNAL

Ref. Attn. — 1.0

Sig. Q — 10

Freq. Trim — 0

The pulse and bias characteristics are:

Quiescent Reverse Bias — 6 Volts

Majority Carrier Pulse Height — -.1 Volts

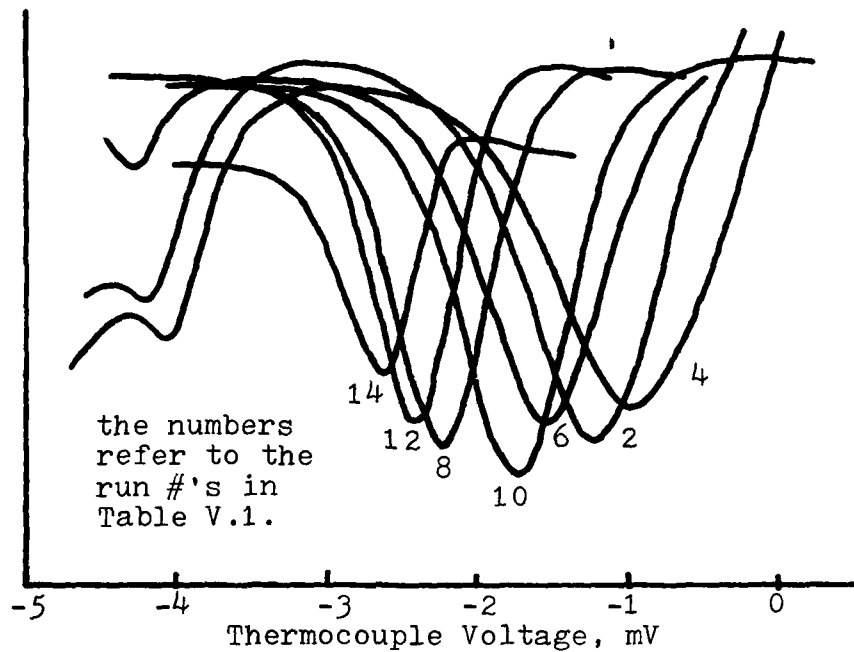
Majority Carrier Pulse Length — .1 msec.

Hold Time — .2 msec.

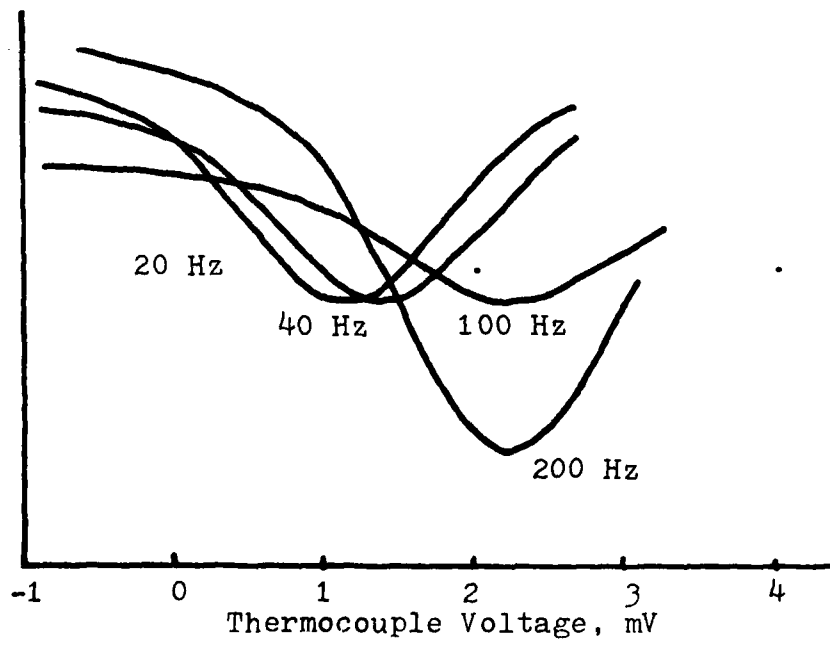
Figure V.1. shows the output of the X-Y recorder for the Si. runs. The vertical axis is the output of the Lock-In Amplifier and the horizontal axis is the Voltage reading of the Thermocouple. The Thermocouple used was a type 'T' Copper-Constantan thermocouple. Table V.1.

details the important parameters of these runs. The emission rate ratio is determined by using Equation (IV-5) with the specified values of  $\tau$ ,  $\tau_1$ , and Lock-In frequency. The actual emission rate window is then the emission rate ratio times the Lock-In frequency.  $T_{max}$  is the computed temperature corresponding to the thermocouple Voltage at which the Lock-In output reaches a local minimum. The values for  $\ln(T_{max}^2/e)$  and  $1/T_{max} \times 10^3$  are then computed. By plotting  $\ln(T_{max}^2/e)$  versus  $1/T_{max}$ , as in Figure V.2., and using Equation (II-11), values for the Energy Level and the prefactor are determined. The procedure is similar for GaAlAs with the results for both shown in Table V.2.

These results are within the range of results presented and discussed by other researchers.<sup>2,4,5</sup>



(a).



(b).

Figure V.1. Lock-In output vs. Thermocouple Voltage for (a). Si. and (b). GaAlAs.

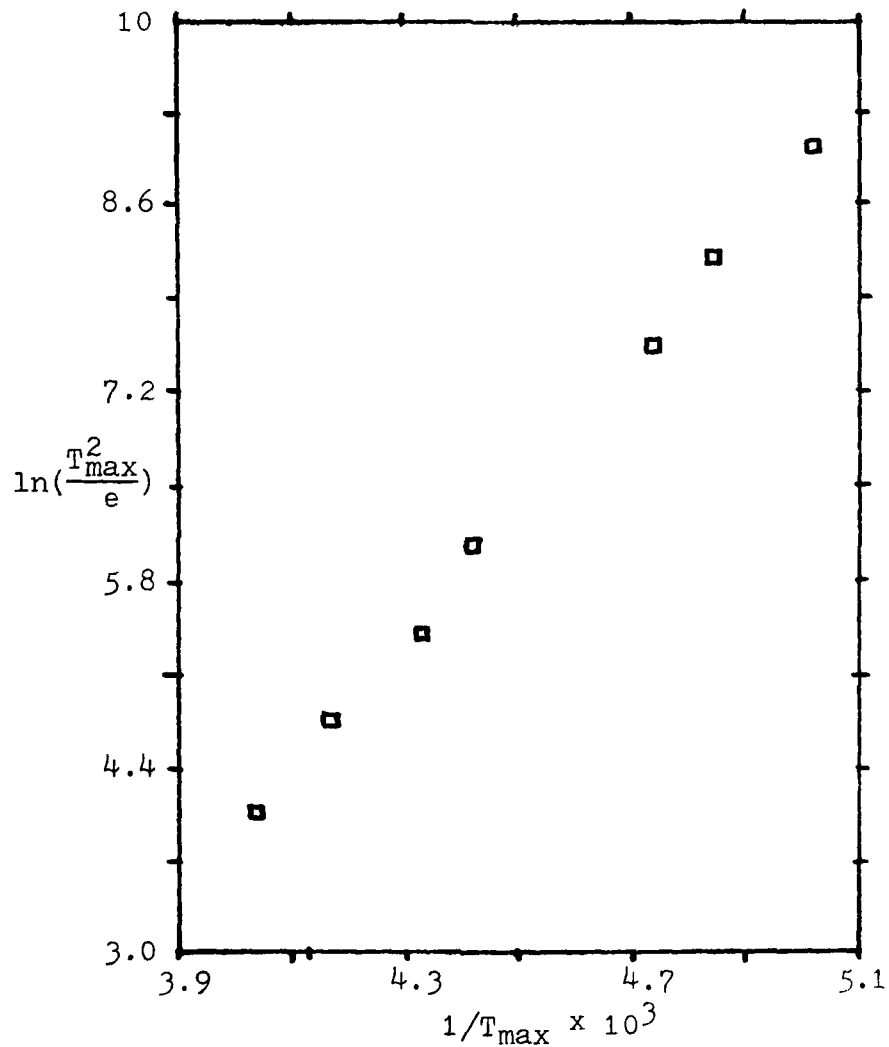


Figure V.2. Plot of  $\ln(T_{\max}^2/e)$  vs.  $1/T_{\max} \times 10^3$  for Silicon.

Run#	Freq.	e	T <sub>max</sub>	ln( $\frac{T_{max}^2}{e}$ )	1/T <sub>max</sub> x 1000	x
2	200Hz	495.5	240K	+4.76	4.17	2.4775
4	400Hz	1033.6	247K	+4.08	4.04	2.584
6	100Hz	241.9	231K	+5.40	4.33	2.419
8	10Hz	23.63	211K	+7.54	4.74	2.363
10	50Hz	119.5	226K	+6.06	4.42	2.389
12	5Hz	11.80	206K	+8.19	4.85	2.36
14	2Hz	4.71	199K	+9.04	5.03	2.355

Table V.1. Observed and Computed data for Silicon runs.

Semiconductor	Energy Level	Prefactor
Silicon	.433 eV	1.11 x 10 <sup>7</sup>
GaAlAs	.590 eV	5.24 x 10 <sup>6</sup>

Table V.2. Results.

### Summary

The study covered by this report was the initial work on what is to be an on going topic of research here at the Naval Academy. This research involves the use of Deep Level Transient Spectroscopy (DLTS) in the study of radiation induced trapping states on semiconductors.

Following an intense study of the systems used by other research teams, I found that I was not able to justify some of the methods which they used. As such I concentrated my efforts on the weaker areas of the experimental technique. Specifically, I developed a new method for describing the operation of the Lock-In Amplifier, and completely redesigned the control circuitry which is the heart of the system. Unfortunately, due to the difficulty (and sometimes impossibility) of obtaining special purpose electronic parts, the redesigned Switch and Control circuit is not yet fully operational. As such, it will be covered by one of the many papers yet to be generated by this continuing research.

The real result of my work was to set up a system of research which will continue indefinitely here at the Academy. This system, continually improving as it is, will continue to make significant contributions in this field of research.

## REFERENCES

1. D. V. Lang, J. App. Phys., 45, 7 (1974).
2. G. L. Miller, D. V. Lang, and L. C. Kimberling, Ann. Rev. Mater. Sci., 377 (1977).
3. D. V. Lang, J. App. Phys., 45, 7 (1974).
4. D. V. Lang, Inst. Phys. Conf. Ser. No. 31, (1977).
5. D. S. Day, M. Y. Tsai, B. G. Streetman, and D. V. Lang, J. App. Phys., 50, 8 (1979).

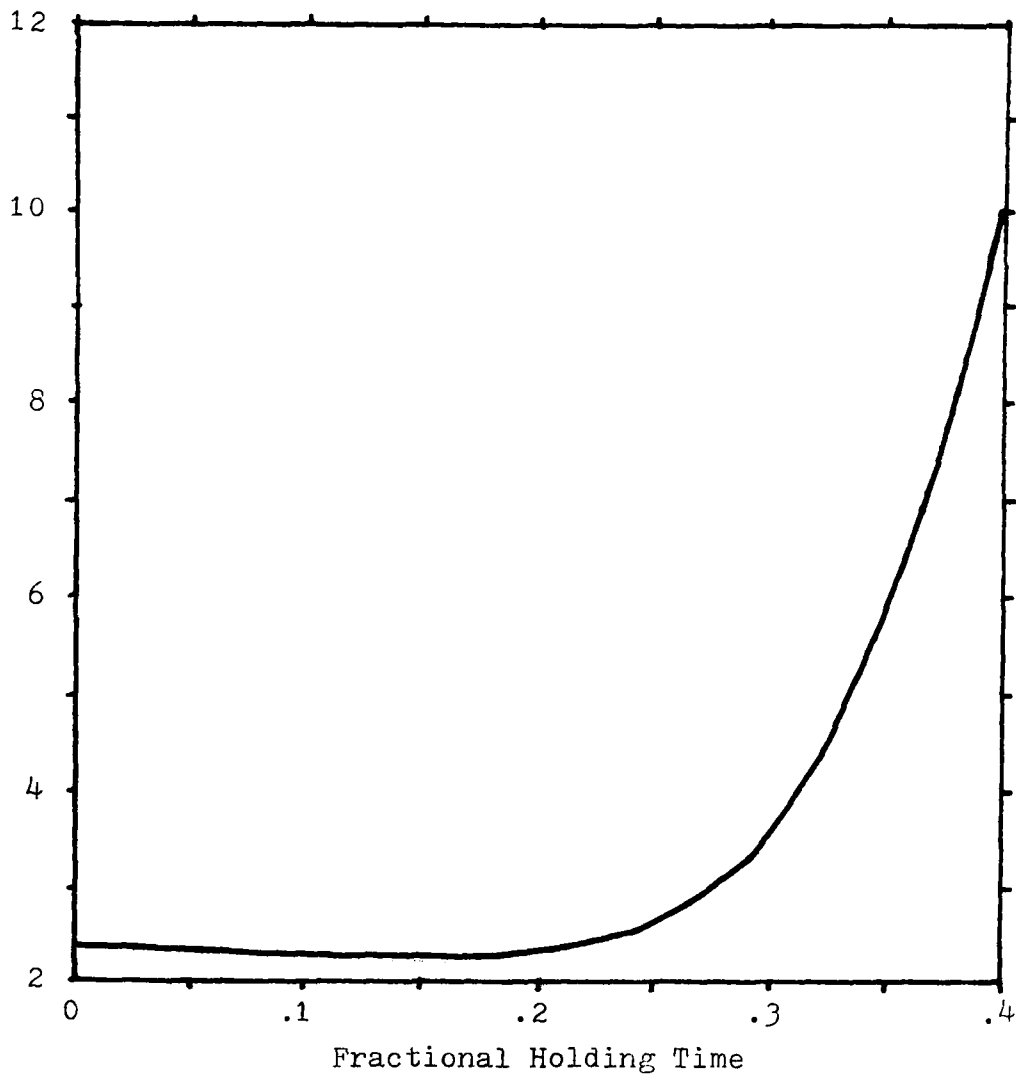


Figure A.1. Plot of Emission Rate Ratio versus Fractional Holding Time for Zero Phase Shift.

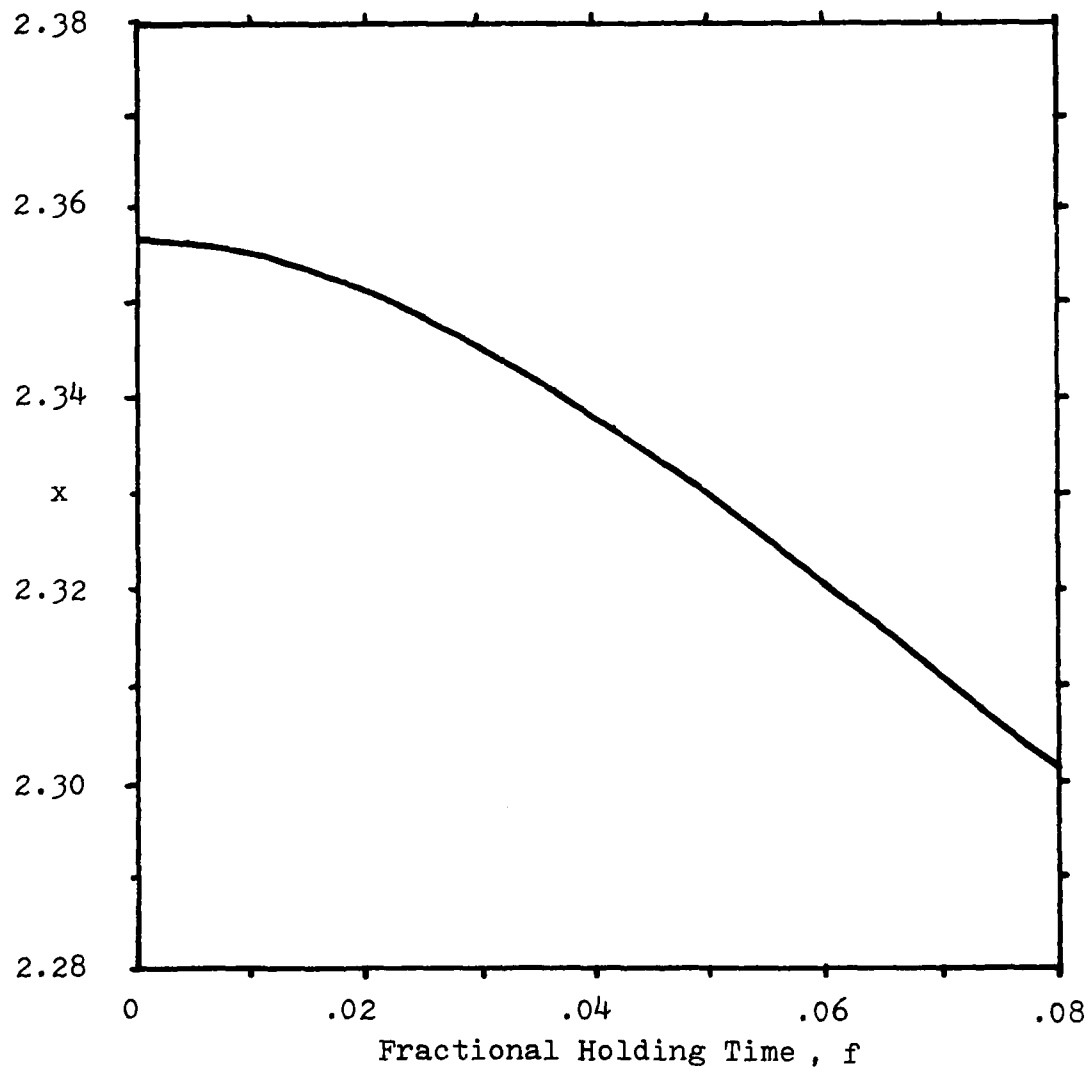


Figure A.2. Plot of Emission Rate Ratio vs. Fractional Holding Time for Phase Shift equals Zero. The formula is a third order fit to the curve.

$$x = 2.3568 - .0538f - 13.186f^2 + 65.793f^3$$

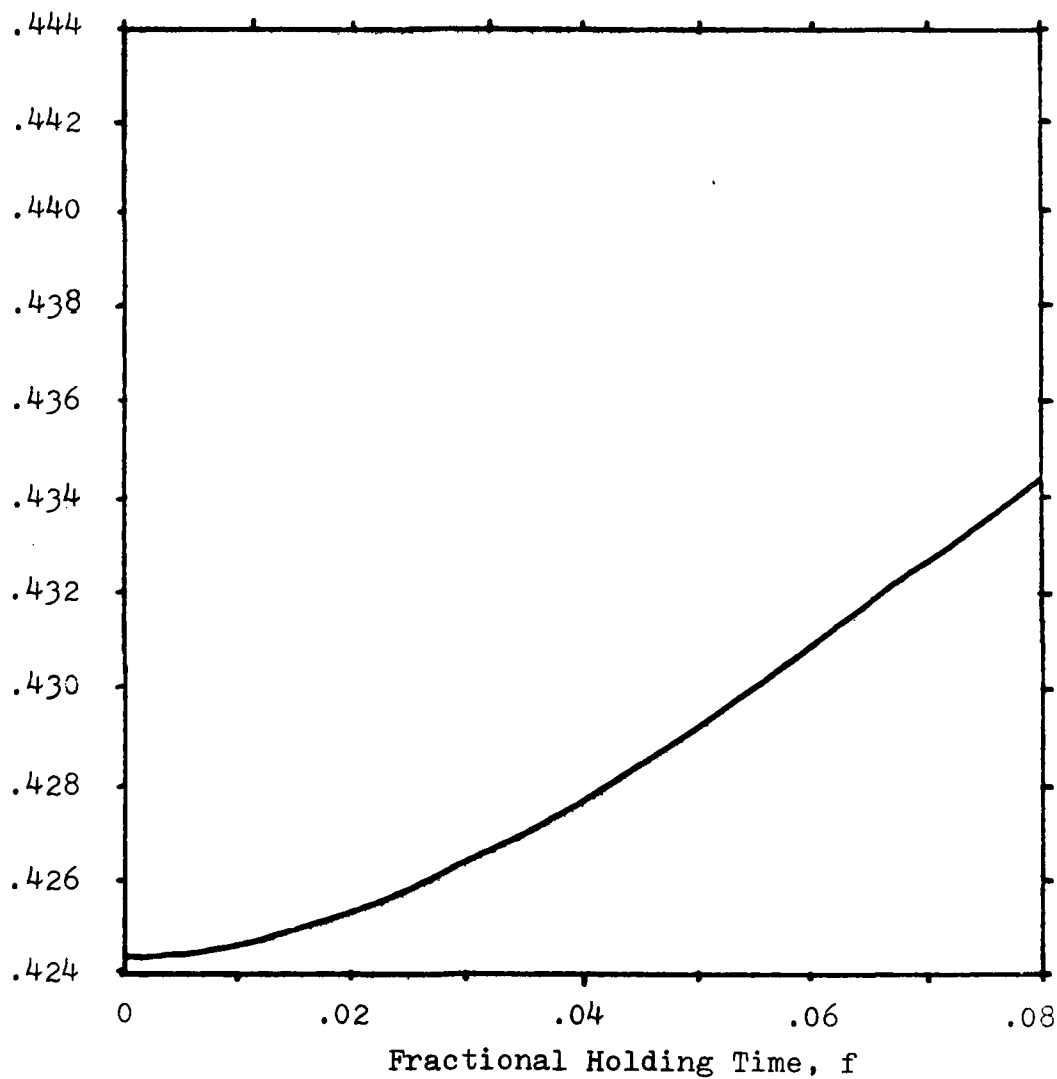


Figure A.3. Plot of Inverse Emission Rate Ratio vs. Fractional Holding Time for Zero Phase Shift. The Formula is a third order fit to the curve.

$$1/x = .424311 + .00837137f + 2.4167f^2 - 11.734f^3$$